Neurobiology of Disease 177 (2023) 106001

Contents lists available at ScienceDirect

Neurobiology of Disease

journal homepage: www.elsevier.com/locate/ynbdi

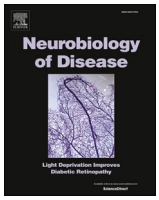

Fibrinogen primes the microglial NLRP3 inflammasome and propagates pro-inflammatory signaling via extracellular vesicles: Implications for blood-brain barrier dysfunction

A.D. Roseborough [a], Y. Zhu [a], L. Zhao [a], S.R. Laviolette [b,c], S.H. Pasternak [d,e], S.N. Whitehead [a,*]

[a] Vulnerable Brain Laboratory, Department of Anatomy and Cell Biology, The Schulich School of Medicine & Dentistry, The University of Western Ontario, London, Ontario, Canada
[b] Addictions Research Group, Department of Anatomy and Cell Biology, The Schulich School of Medicine & Dentistry, The University of Western Ontario, London, Ontario, Canada
[c] Department of Psychiatry, The Schulich School of Medicine & Dentistry, The University of Western Ontario, London, Ontario, Canada
[d] Department of Clinical Neurological Sciences, The Schulich School of Medicine & Dentistry, The University of Western Ontario, London, Ontario, Canada
[e] Robarts Research Institute, The Schulich School of Medicine & Dentistry, The University of Western Ontario, London, Ontario, Canada

ARTICLE INFO

Keywords:
Microglia
Blood brain barrier
Fibrinogen
Extracellular vesicles
Stroke

ABSTRACT

The brain's response to acute injury is characterized by increased permeability of the blood-brain barrier (BBB) and pro-inflammatory microglia signaling, both of which have been linked to poor cognitive outcomes and neurological disease. The damaged BBB has increased leakiness, allowing serum proteins like fibrinogen into the brain, which interacts with local cells in a deleterious manner. At the same time, in response to injury, microglia demonstrate increased NLRP3 inflammasome activity and heightened release of pro-inflammatory cytokines. The relationship between increased fibrinogen uptake and microglial inflammasome signaling in the injured brain has not been well described. In this work, we investigate fibrinogen mediated NLRP3 inflammasome priming of BV-2 cells and primary adult microglia and propose a role for extracellular vesicles (EVs) as propagators of this interaction. Following exposure to fibrinogen microglia significantly upregulate transcription of IL-1β, IL-6, NLRP3 and other pro-inflammatory cytokines which was sustained by repeated fibrinogen exposure. Inhibition of fibrinogen mediated NLRP3 signaling was achieved at the transcriptional and assembly level using cannabidiol (CBD) and the NLRP3 inhibitor MCC950, respectively. EVs released following NLRP3 priming carry IL-1β, IL-18 mRNA and fibrinogen, propagate inflammatory signaling and can be detected in the circulation following BBB disruption in a preclinical stroke model. In conclusion, the interplay between fibrinogen extravasation, microglial NLRP3 signaling, and EV release can perpetuate chronic pro-inflammatory signaling and represents a novel method of inflammatory propagation.

1. Introduction

The blood brain barrier (BBB) is a crucial mediator between the circulatory system and the brain's protected environment. The BBB is comprised of endothelial cells, the endothelial basement membrane, astrocytic end feet and pericytes, which work together to control the entry of substances into the brain and the maintain brain homeostasis (Ballabh et al., 2004; Banks, 2008). Disruptions to the BBB can be acute in nature following neurological injury such as stroke and traumatic brain injury or can involve chronic impairment of its structural and functional integrity (Schoknecht and Shalev, 2012; Hay et al., 2015; Prakash and Carmichael, 2015).

Neuroimaging studies have confirmed that increased permeability of the BBB is a feature of normal aging that is exacerbated by cerebrovascular disease (Viggars et al., 2011; Bridges et al., 2014; Raja et al., 2018; Thrippleton et al., 2019; Verheggen et al., 2020a, 2020b). It also occurs in the early stages of Alzheimer's disease, and is associated with cognitive dysfunction independent of amyloid and tau pathologies (Montagne et al., 2015; Janelidze et al., 2017; Sweeney et al., 2019). BBB dysfunction can result from the loss of endothelial tight junctions,

* Corresponding author at: Department of Anatomy and Cell Biology, 458 Medical Sciences Building, The University of Western Ontario, London, Ontario N6A 3K7, Canada.
E-mail address: shawn.whitehead@schulich.uwo.ca (S.N. Whitehead).

https://doi.org/10.1016/j.nbd.2023.106001
Received 7 September 2022; Received in revised form 20 December 2022; Accepted 12 January 2023
Available online 13 January 2023

retraction of astrocytic end feet, loss of pericytes and degradation of the endothelial basement membrane. At the histological level, disruption to the BBB is evidenced by visible extravasation of serum proteins such as fibrinogen, thrombin and albumin into the brain parenchyma (Viggars et al., 2011; McAleese et al., 2019; Merlini et al., 2019; Roseborough et al., 2021).

Fibrinogen is a circulating coagulation protein that has received recent attention due to its emerging role in neurological diseases (Vilar et al., 2020). Elevated fibrinogen levels are associated with worse neurological outcomes post-stroke and faster cognitive decline in those with mild cognitive impairment (Xu et al., 2008; Lee et al., 2017). In the context of BBB breakdown, fibrinogen exerts deleterious effects on the cells of the brain including reduced neuron density, inhibition of oligodendrocyte maturation and promotion of perivascular microglial activity (Davalos et al., 2012; Petersen et al., 2017; Jenkins et al., 2018; Merlini et al., 2019).

In addition to BBB dysfunction, increases in microglia-mediated pro-inflammatory signaling are another key feature of the damaged brain (Koellhoffer et al., 2017; Raj et al., 2017). In normal aging as well as neurological disease, microglia upregulate the (NLRP3) inflammasome, a key signaling pathway involved in the cleavage and release of the pro-inflammatory cytokine Interleukin-1 Beta (IL-1β) (Ravichandran and Heneka, 2021). Activation of the NLRP3 inflammasome is a two-step process involving an initial stimulus where pattern recognition receptors (PRRs) on microglia recognize ligands that cause transcriptional priming of key pathway components. This is followed by a secondary stimulus leading to full inflammasome assembly, cytokine cleavage and release (Swanson et al., 2019). Another consequence of activation of the NLRP3 inflammasome in microglia is the increased release of extracellular vesicles (EVs), small membrane-bound vesicles that can act as mediators of cell-cell communication (Iraci et al., 2016). Previous in vitro studies have demonstrated that EVs released from activated monocytes and macrophages contain bioactive IL-1β, and these EVs can induce pro-inflammatory responses in neighboring cells (MacKenzie et al., 2001; Zhang et al., 2017; Budden et al., 2021).

The influence of fibrinogen on NLRP3 priming in microglia, and the consequences of subsequent EV release, has not been extensively studied and warrants investigation given the co-occurrence of fibrinogen extravasation and microglia NLRP3 activation in aging. Furthermore, the ability of inhibitors of pro-inflammatory microglia signaling to blunt the effects of fibrinogen exposure have not been studied. Cannabidiol (CBD) is known to inhibit microglia activation through NFκB signaling pathways, whilst MCC950 is a small-molecule inhibitor of NLRP3 inflammasome assembly (Kozela et al., 2010; Coll et al., 2015).

Here, we sought to investigate the in vitro dynamics, and inhibition of, fibrinogen-mediated NLRP3 inflammasome priming in BV-2 microglia and primary adult microglia. We confirmed the role of microglia EVs in the propagation of pro-inflammatory signaling following fibrinogen exposure. Finally, we demonstrate that microglia EVs containing fibrinogen are shed into the blood following endothelin-induced stroke.

2. Methods

2.1. Cell culture

Cell growing conditions: BV-2 cells were donated from Dr. Tuan Trang at the University of Calgary. BV-2 cells were cultured at 37 °C in a humidified atmosphere with 5% CO_2. Cells were maintained in Dulbecco's Modified Eagle Medium (DMEM) (Gibco) supplemented with 10% fetal bovine serum, Penicillin (100 U/mL) and Streptomycin (100 μg/mL) (Gibco).

2.2. Primary microglia isolation

Adult microglia were isolated from 12-month old Fischer rats following a modified version of a Percoll isolation method (Agalave et al., 2020). Rats were euthanized using an overdose of pentobarbital prior to decapitation and isolation of the brain which was dissected from the cerebral vessels and meninges. After mechanical dissociation the tissue was passed through a 70 μm strainer and resuspended in 75% Percoll. A 70–50-35% Percoll gradient was established and centrifuged at 2000xG for 20 min without break. The band of cells appearing at the 70–50% Percoll interface was collected, washed once with PBS and seeded at a density of 2×10^5 cells per well of a 24-well plate. Cells were maintained in DMEM-F12 culture medium supplemented with 10% fetal bovine serum, Penicillin (100 U/mL) and Streptomycin (100 μg/mL).

2.3. Cell treatments

Cell seeding: BV-2 cells were seeded in 24-well plates at a density of 1.7×10^5 cells/well for RNA collections or 12-well plates at 3.4×10^5 cells/well for supernatant and cell lysate collections. Eight hours prior to treatment cells were washed with PBS and maintained in serum free media. Fibrinogen treatment: Cells were treated with fibrinogen (Sigma) at a range of doses from 0.01 mg/mL to 1 mg/mL for 3–12 h. For all experiments after the initial fibrinogen dose testing a concentration of 0.1 mg/mL was used to limit thickening of the media. For experiments with repeated fibrinogen treatments, cells were treated with fibrinogen at baseline and again at 3 & 6 h or 6 h only. CBD pre-treatment: CBD (Tocris, 1570) was reconstituted in DMSO at 50 mM. To determine the dose of CBD sufficient to inhibit pro-inflammatory signaling cells were pre-treated with CBD prior to LPS exposure (500 ng/mL) (Fig. S1). 3 h prior to fibrinogen exposure cells were treated with CBD at a concentration of 0.5 μM with a final concentration of 0.001% DMSO. ATP & MCC950 treatment: After 2.5 h of fibrinogen exposure, cells were treated with MCC950 (1 uM) for 30 min followed by ATP (2 mM). After ten minutes supernatants (500 μL) were collected, and cells were lysed using RIPA buffer with additional phosphatase and protease inhibitors (Roche Custombiotech). EV treatment: BV-2 cells were treated with EVs at concentration of 2000–12,000 EVs/cell for 3 h prior to RNA collection. For all experiments involving EV isolation or treatment cells were cultured in EV-depleted FBS that was ultra-centrifuged at 100,000xG 4 °C overnight after which the supernatant was filtered through a 0.2 μm filter.

2.4. RNA isolation and qPCR

RNA was isolated from cells using TRIzol (Life Technologies) mediated extraction as previously described. RNA was isolated from EVs using miRNeasy Micro Kit (Qiagen, cat # 217084) according to manufacturer's protocol. Following extraction, RNA concentrations were determined using a Nanodrop One spectrophotometer (Thermo Fisher Scientific) Quantitative real time PCR (qPCR): cDNA was synthesized using 2 μg of RNA from each cell sample and 1 μg of RNA from EV samples. Target gene amplification was performed with specific forward and reverse primers designed using the NCBI primer design tool. Primer sequences and GenBank accession numbers are provided in Supplemental Table 1. Two μL of cDNA was combined with forward and reverse primers (at 125 nM each) and SsoAdvanced Universal SYBR Green Mix (Bio-Rad). RPL13α was used as an endogenous control with all mRNA expression levels normalized to this value. Comparison of transcription levels was performed using the $\Delta\Delta C^T$ method (Livak and Schmittgen, 2001).

2.5. ELISA

Supernatant (500 μL) was collected from each well of BV-2 cells seeded in a 12-well plate after either 12 h of fibrinogen exposure or 3 h of fibrinogen exposure (0.01–0.1 mg/mL) followed by 30 min of ATP exposure. Supernatant were centrifuged at 500xG for 5 min at 4 °C and immediately analyzed in duplicates using a mouse IL-1β ELISA (proteintech, KE10003) kit according to manufacturer's instructions.

2.6. Western blotting

Lysates: Cell lysates were sonicated and centrifuged at 15,000xG for 10 min at 4 °C. The protein concentration of the resulting supernatant was determined using a BCA protein assay kit (Pierce, Thermo Fisher Scientific) performed according to the manufacturer's instructions. Protein (15 μg per sample) was diluted in loading buffer (1× LDS, 5 mM DTT in 0.5% SDS). Supernatant precipitations: protein from supernatants (500 μL) were precipitated using the following protocol: Equal volume methanol and ¼ volume chloroform were added to the sample, vortexed and centrifuged at 13000xG for 5 min at 4 °C. The upper aqueous phase was discarded, and methanol (equal to starting volume) was added to the sample and vortexed prior to centrifugation at 13000xG for 5 min at 4 °C. The supernatant was discarded, and protein pellet was dried for 10 min at 55 °C, resuspended in loading buffer (1× LDS, 5 mM DTT in 0.5% SDS) and vortexed vigorously. Proteins from cell lysates and supernatant precipitates were denatured at 95 °C for 5 min and separated using gel electrophoresis of Bis-Tris 10% acrylamide gels in MOPS SDS running buffer (Thermo Fisher Scientific) at 70 mA per gel, followed by transfer to a PVDF membrane (Roche Diagnostics) at 100 V for 100 min on ice. After transfer the membrane was washed briefly in TBST (0.1% Tween) and blocked overnight at 4 °C with 5% milk in TBST. After blocking the membranes were washed briefly in Tris Buffered Saline-Tween 20 (TBST) (Tris-HCl 50 mM pH 8.0, NaCl 0.15 M, Tween 20 0.1% *v*/v) and incubated with the following primary antibodies in 5% BSA in TBST for one hour at room temperature: Caspase-1 (1:1000, Cell Signaling Technology, D7F10), cleaved Caspase-1 Asp297 (1:1000, Cell Signaling Technology, D57A2). Membranes were washed 3 x for 10 min with TBST and incubated with donkey anti-rabbit HRP-conjugated secondary antibodies (1:10,000, Jackson Laboratories) for one hour at room temperature. Finally, membranes were washed 3 x for 10 min with TBST prior to detection with chemiluminescent HRP substrate (Immobilon) and imaging using a ChemiDoc MP system (Bio-Rad).

2.7. Preclinical stroke model

Animal care: All animal procedures were approved by the Animal Care Committee at Western University (protocol 2018–132). All rats used in this study were housed in facilities maintained by Western University Animal Care and Veterinary Services. Surgeries: Sixteen 3-month-old male Fischer344 rats were randomly assigned to either surgery ($n = 8$) or sham (n = 8) groups. Animals were anesthetized using 3% isoflurane and maintained at 1.5% isoflurane with body temperature maintained at 37 °C. Either saline (3 μL) or saline containing Endothelin-1 (600 pmol in 3 μL) was injected into the right dorsal striatum. Euthanasia & brain collection: Animals were euthanized 28 days post-surgery using an intraperitoneal injection of pentobarbital and transcardial perfusion of 180 ml 0.01 M PBS followed by 300 ml 4% paraformaldehyde (PFA) (pH 7.4). Brains were removed and stored in 4% PFA for 24 h, transferred to 30% sucrose for 36 h at 4 °C prior to being cut into either 10 or 30 μm coronal sections using a cryostat (Cryostar NX50, Thermo Fisher Scientific). Blood collection: Terminal 28-day blood was collected from the left ventricle at the time of euthanasia. Plasma was isolated using two rounds of centrifugation at 2500 *g* for 15 min at 4 °C and stored at −80 °C prior to nanoflow analysis.

2.8. Nanoflow cytometry

Incubations: Triplicate aliquots of 10 μL of platelet poor rat plasma and the following antibodies were incubated at room temperature for 30 min: anti-TMEM119 Coralite-647 (100 ng/sample, Proteintech 66,948), anti-Fibrinogen Alexa Fluor-488 (200 ng/sample, Bioss 1240R). All incubations had a final concentration of 0.0125% Triton-X-100 to permeabilize EVs and minimize lysis.(Osteikoetxea et al., 2015) After incubation, samples were diluted 50-fold and triplicates of each incubation were run on the Apogee A60 Micro plus Nanoflow Cytometer (Apogee Flow Systems Inc). Instrument settings: Sheath pressure: 150 mbar, flow rate: 150 μL/min for 130 μL, lasers: 100 mW 405 nm (violet), 70 mW 638 nm (red),70 mW 488 (green). Light scatter of events was produced using the 405 nm laser, with thresholds to eliminate background noise of 34 a.u. for small angle light scatter (SALS) and 21 a.u. for long angle light scatter (LALS). Photomultiplier tube (PMT) voltages: LALS (265 V) SALS (340 V) L488-Grn (525 V) L638-Red (650).

2.9. EV isolation & quantification

Cells were grown in T75 flasks in media supplemented with EV-depleted FBS prior to experiments. 8 h prior to treatment media was exchanged to serum free media after which the media was exchanged again to serum free media with or without fibrinogen (0.05 mg/ml or 0.1 mg/mL) for 12 h. The collected supernatant containing fibrinogen was incubated with thrombin (16 units/mg of fibrinogen) for 10 min at 37 °C. The supernatant was centrifuged at 15,000 *g* for 10 min at 4 °C to remove fibrinogen aggregates and cellular debris. The supernatant was then filtered through 0.2 um nitrocellulose filters (Thermo Fisher Scientific) and concentrated using 100 kDa centrifugal filter units (Amicon, Ultra-15). The concentrated supernatants were ultra-centrifuged at 100,000 *g* for 1 h and 15 min at 4 °C after which the pellet was washed once and resuspended with PBS. Resuspended EVs were diluted 60-fold in PBS prior to quantification using nanoflow cytometry with the same instrument settings listed above. The events/uL was used for determination of EV concentrations for cell treatments.

2.10. Immunocytochemistry

For fibrinogen ICC BV-2 cells were seeded in on glass coverslips (Fisher Scientific) in 24-well plates. After 12 h of fibrinogen exposure, BV-2 cells were fixed for 20 min with 2% formaldehyde followed by three five-minute PBS washes. For tissue staining, 10 μm sections were pre-mounted onto slides. Coverslips/slides were blocked for 1 h at room temperature using PBS with 10% goat serum, 1% Triton-X-100 and 1% Tween. Coverslips/slides were then incubated overnight at 4 °C with the following primary antibodies in blocking solution: anti-fibrinogen (1:200, abcam ab34269), anti-TMEM119 Alexa Fluor 647 (1:500, Proteintech CL-64766948). After three 5-min PBS washes coverslips were incubated with goat anti-rabbit Alexa Fluor 488 conjugated secondary antibody (1:100, Thermofisher #35552) in blocking solution for one hour at room temperature. After another three 5-min PBS washes, coverslips were sealed onto slides using DAPI aqueous mounting medium (Sigma).

2.11. Microscopy

Slides were visualized using brightfield and fluorescent microscopy (Nikon Eclipse Ni-E, Nikon DS Fi2 colour camera, Nikon DS Qi2 fluorescent camera, NIS Elements Imaging) and example images were captured using 10× and 20× objectives.

2.12. Statistical analyses

All statistical analysis was performed using Graphpad Prism 8 software. Group comparisons were performed using unpaired Student's *t*-test, One-Way ANOVA or Two-Way ANOVA with significance value of $p = 0.05$.

3. Results

3.1. NLRP3 inflammasome priming in response to fibrinogen is dose-dependent

To investigate the effects of fibrinogen on pro-inflammatory microglia signaling we treated BV-2 microglia with increasing doses of

fibrinogen for 3–12 h. Following fibrinogen exposure, BV-2 microglia significantly upregulate IL1-β, IL-6 and NLRP3 transcription in a dose-dependent manner (Fig. 1A). All doses of 0.05 mg/mL and above were sufficient to cause upregulation of IL1- β transcription after 3 h, doses of 0.1 mg/mL and above retained IL1- β upregulation after 6 h. Only 1 mg/mL resulted in a sustained response 12 h post-exposure ($p = 0.0137$). Repeated exposure to fibrinogen (0.1 mg/mL) every 3 or 6 h after the initial treatment resulted in sustained IL1- β upregulation at 9 h in comparison to a single exposure (Fig. 1C). To determine whether release of IL-1β into supernatant was dependent on full NLRP3 assembly we measured IL-1β concentrations after fibrinogen exposure with subsequent ATP exposure or extended fibrinogen exposure alone. After three hours of fibrinogen exposure followed by stimulation with ATP, 0.1 mg/mL of fibrinogen was the minimum dose that induced increased IL-1β

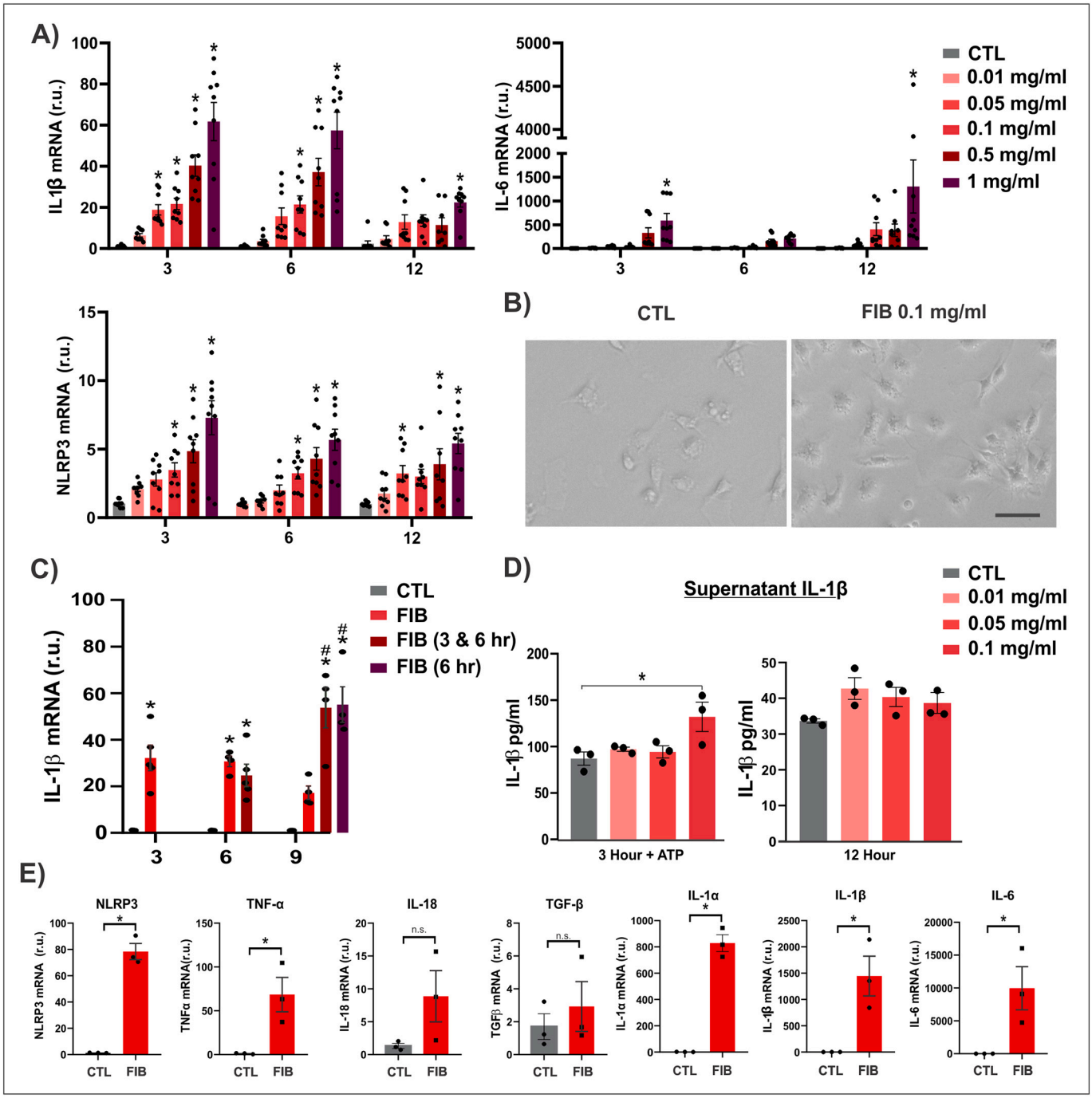

Fig. 1. Fibrinogen is a potent activator of the NLRP3 inflammasome in BV-2 microglial cells and primary adult microglia. A) qPCR measurement of IL-1β, IL-6 and NLRP3 expression in BV-2 microglia following exposure to fibrinogen (0.01–1 mg/mL) for 3, 6 and 12 h. *Indicates statistical difference from control B) Photo micrographs of primary adult microglia following exposure to fibrinogen (0.1 mg/mL) for 6 h C) qPCR measurement of IL-1β expression in BV-2 microglia after a single fibrinogen exposure, or repeated exposure every 3–6 h. * Indicates significant difference from control, # indicates significant difference from single fibrinogen treatment. D) IL-1β in supernatants measured using ELISA after either 3 h fibrinogen exposure with secondary ATP exposure (2 mM) for 30 min, or fibrinogen exposure alone for 12 h. E) qPCR measurements of IL-1α, IL-1β, IL-6, NLRP3, TNF-α, IL-18 and TGF-β expression in primary adult microglia collected from 12-month wildtype Fisher rats following 6 h of fibrinogen exposure (0.1 mg/mL). Statistical comparisons were performed using Two-Way ANOVA or unpaired Student's *t*-test where appropriate with significance threshold of $p < 0.05$.

release ($p = 0.0374$) (Fig. 1D). In the absence of ATP, prolonged fibrinogen exposure alone did not result in increased release of IL-1β (Fig. 1D). Since BV-2 cells differ in their upregulation of pro-inflammatory cytokines in comparison to primary microglia (Horvath et al., 2008), we also treated primary microglia isolated from 12-month-old rats. In response to fibrinogen, primary adult microglia display enlarged cell bodies and form clusters (Fig. 1B). After 6 h of fibrinogen exposure there is significant upregulation of IL-1α ($p = 0.0002$), IL-1β ($p = 0.0187$), NLRP3 ($p = 0.0002$), IL-6 ($p = 0.0388$) and TNF-α ($p = 0.0266$) while TGF- β and IL-18 were not significantly altered (Fig. 1D).

3.2. Inhibition of NLRP3 inflammasome at the level of transcription and assembly

Using LPS treatment we first determined that 0.5 μM of CBD prior to LPS exposure was sufficient for significant inhibition of pro-inflammatory transcriptional priming (Fig. S1), as has been previously reported (Kozela et al., 2010). Three-hour pre-treatment with CBD significantly reduced transcriptional upregulation of IL1-β ($p = 0.0003$), IL-6 ($p = 0.0053$) and NLRP3 ($p = 0.0011$) in response to three hours of fibrinogen exposure (Fig. 2A). After 6 h of fibrinogen exposure, significant inhibition of IL1-β ($p = 0.0178$) and IL-6 ($p = 0.0265$) upregulation was maintained, however NLRP3 was no longer significantly reduced by CBD pre-treatment (Fig. 2A). Following fibrinogen priming and ATP treatment, a significant increase in the release of cleaved caspase-1 into supernatant was observed ($p = 0.0347$), indicative of full NLRP3 inflammasome assembly (Fig. 2B). This process was significantly inhibited by the addition of the small-molecule inhibitor MCC950 30 min prior to ATP stimulation (Fig. 2 B—C).

3.3. Fibrinogen, IL-1β and IL-18mRNA are carried by pro-inflammatory microglial EVs

To investigate how fibrinogen-mediated microglia signaling is propagated we measured fibrinogen within EVs released from fibrinogen-exposed microglia. Immunocytochemistry demonstrates fibrinogen labeling of BV-2 microglia 12-h following fibrinogen exposure. In EVs isolated from microglia culture medium, nanoflow cytometry (Fig. 3C) confirmed the presence of fibrinogen. Isolated EVs from fibrinogen exposure cells also carried pro-inflammatory mRNA transcripts reflective of NLRP3 priming. IL-18 and IL-1β mRNA levels and were significantly higher in EVs released from fibrinogen-exposed cells than control cells ($p = 0.027$ and $p = 0.0075$, respectively). To examine the cell-cell signaling capability of microglia EVs naïve microglia were treated with varying doses of EVs (2000–12,000/cell) collected from cells exposed to fibrinogen at either 0.05 mg/ml or 0.1 mg/ml. Treatment with EVs induced upregulation of IL1-β transcription which was enhanced by treatment with a higher number of EVs or higher dose of fibrinogen to the donor cell (Fig. 3E). At a dose of 0.05 mg/mL to the donor cells, 12,000 EVs/ cell induced significant IL1-β upregulation in the naïve recipient cells ($p = 0.0027$). At a dose of 0.1 mg/ml, 4000 EVs/ cell were sufficient to induce significant upregulation of IL1-β in the naïve recipient cells ($p = 0.0218$) which was enhanced when the EV concentration was increased to 8000 EVs/cell ($p = 0.0002$) or 12,000 EVs/cell ($p = 0.0001$).

3.4. Fibrinogen in microglia EVs can be detected in peripheral circulation

Using a preclinical stroke model, with confirmed BBB dysfunction (Fig. 4A), we measured the presence of fibrinogen in circulating EVs. Brains were collected for histology and plasma was analyzed by nanoflow cytometry assessments 28 days after either saline or endothelin-1 injection into the dorsal striatum to induce a focal ischemic injury.

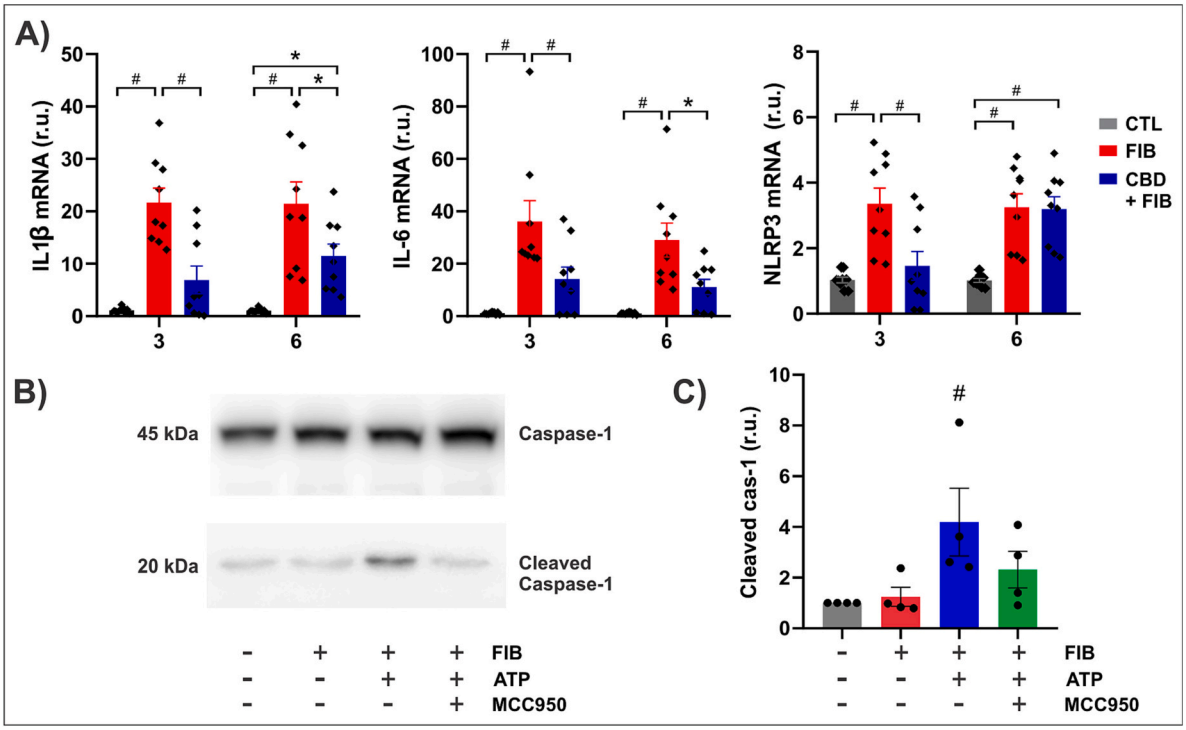

Fig. 2. Fibrinogen mediated activation of the NLRP3 inflammasome is inhibited at the level of transcription of NLRP3 assembly. A) qPCR measurement of IL-1β, IL-6 and NLRP3 following exposure to fibrinogen for 3–6 h with or without 3-h pre-treatment with CBD (0.5 μM). B) Western blot of Caspase-1 in cell lysates and cleaved Caspase-1 from supernatants following exposure to fibrinogen for 3 h followed by addition of ATP (2 mM) for 10-min with or without MCC950 (1 μM) treatment 30 min prior. C) Quantification of cleaved Caspase-1 in supernatants, normalized to full-length Caspase-1. Group comparisons performed using One- or Two-Way ANOVA where required, # indicates statistical significance with $p < 0.01$, * indicates $p < 0.05$.

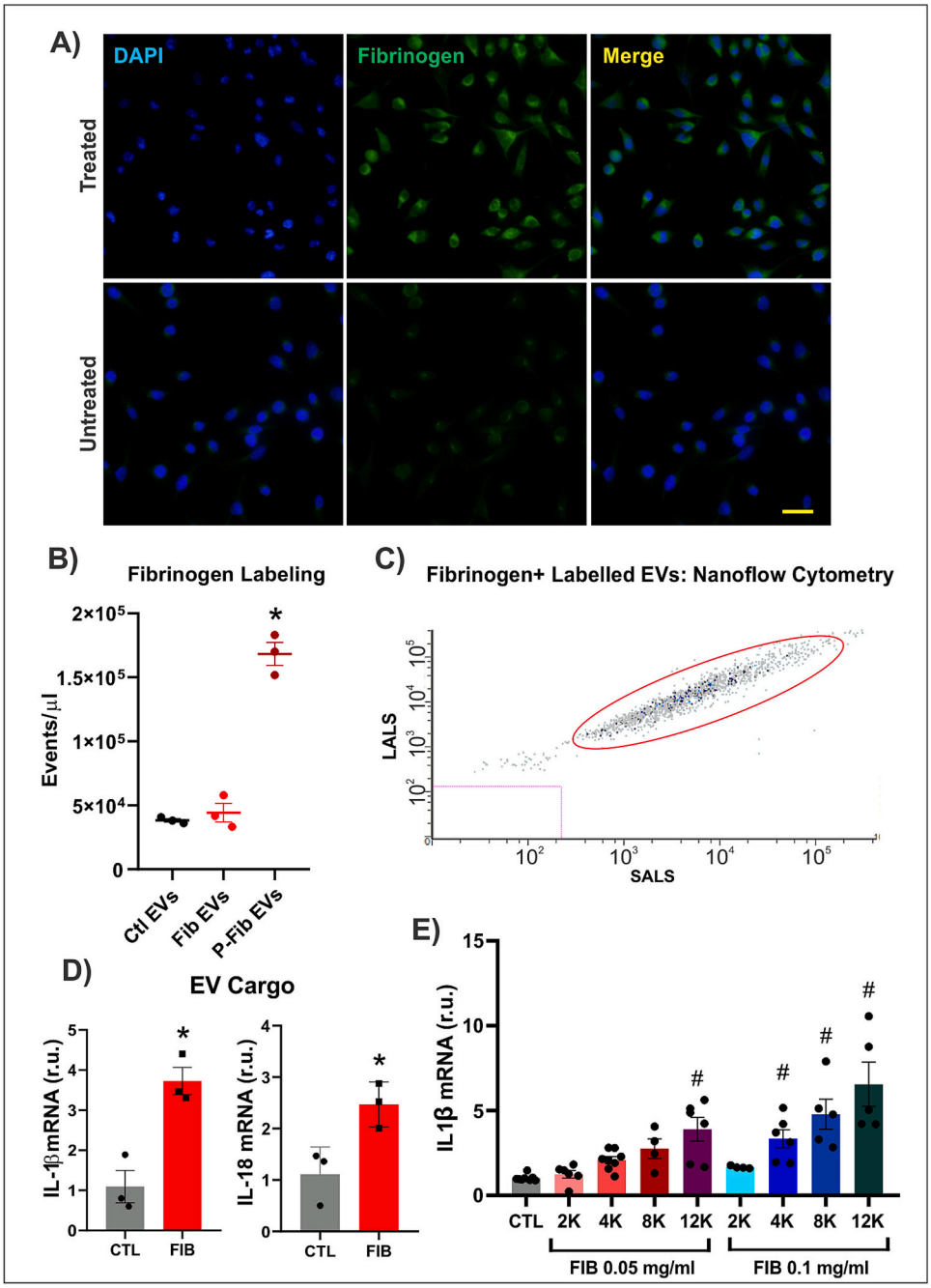

Fig. 3. Fibrinogen is detected in pro-inflammatory extracellular vesicles released from microglia after NLRP3 priming. A) Immunofluorescent staining of fibrinogen in BV-2 microglia 12-h following fibrinogen exposure (0.1 mg/mL) B) Quantification of fibrinogen labelled EVs isolated from BV-2 microglia supernatant using Apogee A60 Plus Nanoflow cytometer after incubation with AF-488 conjugated fibrinogen antibody. P-Fib EVs were permeabilized with 0.05% Triton-X-100C) Example light scatterplot of fibrinogen-labelled EVs measured using nanoflow cytometry and gated to display only 488-fluorescently labelled D) qPCR measurement of IL-1β and IL-18 mRNA levels in EVs isolated from BV-2 microglia supernatant after 12-h with or without fibrinogen exposure E) qPCR measurement of IL-1β following 3 h of treatment with EVs (2000–12,000/cell) isolated from microglia exposed to fibrinogen (0.05 mg/mL or 0.1 mg/mL) and applied to naïve microglia.

Nanoflow cytometry confirmed an increase in plasma EVs that were fluorescently co-labelled with both fibrinogen and TMEM119 in the stroke animals (16,771 ev/µL ± 2432) in comparison to saline injected animals (9076 ev/µL ± 936.4, $p = 0.0205$) (Fig. 4B). Immunofluorescence demonstrates the accumulation of fibrinogen within TMEM119+ microglia in the injury site (Fig. 4C).

4. Discussion

Given the overlap of BBB dysfunction and pro-inflammatory microglia activity in acute neurological disease, including stroke, it is imperative to gain a better understanding of the interactions between these two phenomena. The list of molecules that initiate NLRP3 priming is highly diverse, and stimuli characteristic of proteinopathies such as β-amyloid or α-synuclein represent instigators of the microglia NLRP3 inflammasome in the context of AD and PD, respectively (Ravichandran and Heneka, 2021). We therefore hypothesized that fibrinogen could similarly act as a primer of the microglia NLRP3 inflammasome in the context of disease-related increases in BBB leakiness.

Our findings demonstrate for the first time that fibrinogen is indeed a potent primer of the microglial NLRP3 inflammasome in a dose-dependent manner. Given that the normal range of plasma fibrinogen concentrations is 1.5–4 mg/ml, this work demonstrates that microglia are sensitive to doses of fibrinogen 20-40× lower than circulating plasma levels (Vilar et al., 2020). The response to fibrinogen was short-lived and within 9 h of treatment significant upregulation of IL-1β was lost. However, repeated treatments of fibrinogen could sustain NLRP3 priming for a longer duration. Fibrinogen alone was insufficient to elicit increased release of mature IL-1β within 12 h suggesting that its main effects occur at the level of transcriptional priming. However, following secondary ATP exposure fibrinogen-mediated transcriptional priming did result in increased IL-1β release. This suggests that prolonged

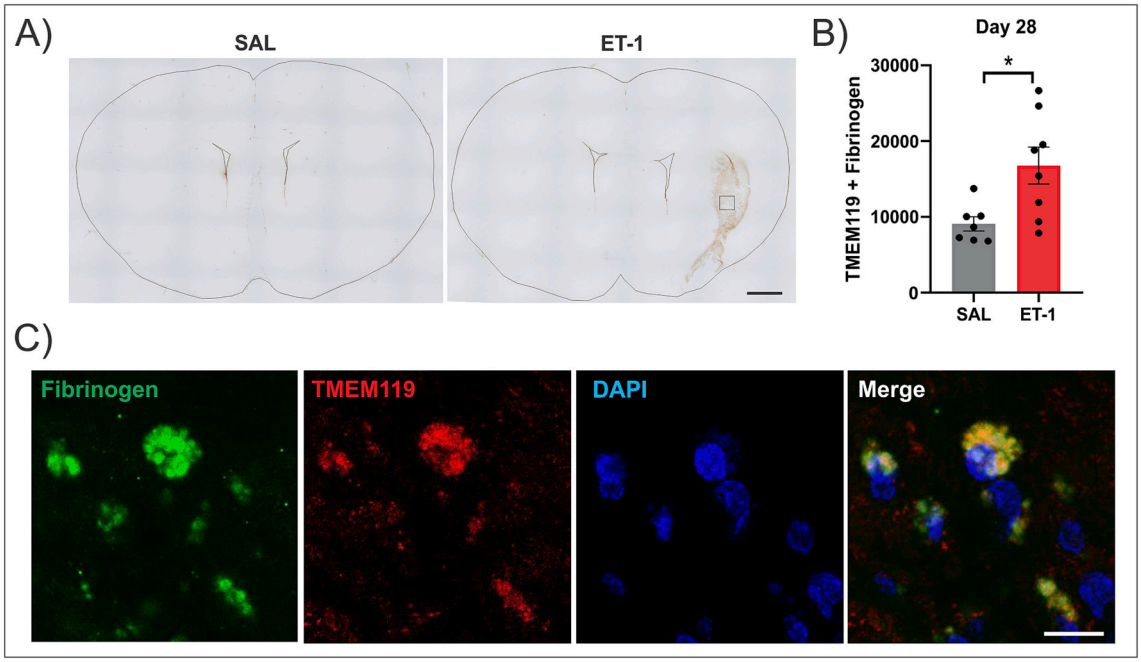

Fig. 4. Fibrinogen is detected within circulating microglial EVs in an experimental model with blood-brain barrier dysfunction. A) IHC of anti-rat IgG using sections from saline or ET-1 injected brains 28 post-surgery. The lateral ventricles and outer edge of the tissue have been outlined to improve visualization of tissue. Box indicates anatomical location of IF images presented in C. Scale bar indicates 500 μm. B) Nanoflow cytometry detection of AF-647+/TMEM119+ and AF-488 fibrinogen co-labelled events/μL of plasma collected 28 days from either saline or ET-1 injection groups. C) Immunofluorescence labelling of fibrinogen and TMEM119 in the injury site 28-days post-stroke. Images taken at 60× magnification, scale bar indicates 25 μm.

extravasation of serum proteins resulting from BBB leakiness following neurological injury may impact priming of microglia NLRP3 inflammasome activity and alter release of mature IL-1β once full assembly occurs. Whether these results translate in vitro to models of neurological injury that provide the second stimulus for full NLRP3 assembly and cytokine release, such as ATP or K+ release from nearby dying cells, requires further study.

Since aging affects the response of microglia to pro-inflammatory stimuli, and many neurological insults like stroke occur in midlife, we chose to validate our findings using microglia isolated from 12-month rats. Previous work from our group has demonstrated increases in pro-inflammatory microglia in the white matter of rats at this age-point, which is a brain region vulnerable to BBB breakdown and fibrinogen extravasation (Montagne et al., 2018; Levit et al., 2021; Roseborough et al., 2021). In this study, adult primary microglia demonstrate a much more robust response to fibrinogen than BV-2 cells, highlighting a limitation in the use of BV-2 cells for modelling microglia activation. After fibrinogen exposure, adult microglia with enlarged cell bodies cluster and demonstrate upregulation of pro-inflammatory transcripts (IL1-a, IL1-B, NLRP3, TNF-a, IL-6) while TGF-β, often considered neuroprotective when expressed by microglia, was not significantly changed. This is in contrast to the upregulation of astrocyte-derived TGF-β signaling during BBB breakdown, highlighting the cell-specific responses of glial cells to BBB dysfunction (Senatorov et al., 2019). Future work on primary microglia from different ages, and the incorporation of mixed culture models is required to better understand the effects of age and cellular environment on the microglia response to fibrinogen.

The consequences of increased pro-inflammatory cytokine release by microglia include leukocyte recruitment, decreased endothelial tight junctions and breakdown of the endothelial basement membrane (Feuerstein et al., 1994). Thus, fibrinogen extravasation into the brain following acute ischemia may result in a negative cycle whereby the priming of microglia produces additional pro-inflammatory mediators that further compromise BBB integrity. Therapeutic strategies are required that can dampen ongoing microglia priming, either via reduction of fibrinogen, which has been shown to improve microgliosis in models of AD and Multiple Sclerosis (Ryu and McLarnon, 2009), or via direct manipulation of inflammasome pathways. Since NLRP3 inflammasome requires two steps, transcriptional priming and then assembly and cleavage of cytokines by cleaved caspase-1, we investigated inhibition of this pathway at both levels. CBD has been previously reported to inhibit LPS-induced NFκB signaling via JAK/STAT pathways (Kozela et al., 2010) whilst MCC950 is a small-molecule inhibitor of NLRP3 assembly that has improved outcomes in preclinical models of stroke and AD (Dempsey et al., 2017; Ismael et al., 2018). In this study both CBD and MCCC950 were successful in attenuating either fibrinogen-mediated priming of the NLRP3 inflammasome or the release of cleaved-caspase 1 following NLRP3 assembly in vitro. Whether previously reported improvements in stroke volume and edema achieved via MCC950 inhibition are also attainable by inhibition of fibrinogen mediated NLRP3 signaling is an important future direction. Incorporation of pharmacological inhibition of the NLRP3 inflammasome in vivo using preclinical models of BBB dysfunction will elucidate the potential benefits of blunted fibrinogen-mediated microglia priming.

EVs have emerged as key effectors of cell-cell communication in neurological disease and following NLRP3 activation of macrophagic cells (Zhang et al., 2017). This is largely due to their ability to carry both disease-specific cargo, such as tau or α-synuclein, and pro-inflammatory mediators including cytokines, miRNA, and mRNA molecules. For the first time to our knowledge, we demonstrate that EVs generated from microglia following fibrinogen exposure propagate NLRP3 priming to naïve cells in a dose-dependent manner. EVs isolated from fibrinogen exposed microglia carried both IL-1β and IL-18 mRNA, reflecting their ability to propagate molecules implicated in NLRP3 inflammasome priming from one cell to another. The type of EV responsible for signal propagation in our model can't be confirmed using our isolation method, representing a limitation of this work and an important outstanding question. Future work is needed to better understand the biology underlying the release of fibrinogen in EVs whether it be from cell-membrane derived vesicles or processing through the endosomal-

lysosomal pathway and secretion in exosomes. It is also unknown whether the fibrinogen is carried exclusively within EVs as cargo or bound to the surface. Although our nanoflow cytometry results show an increase in labeling after permeabilization of the EVs, suggesting that a proportion of EV-fibrinogen is within the vesicles, it is likely that surface binding is occurring as well given that microglia are known to express the fibrinogen binding protein Cd11c, Cd11b as well as others (Nham, 1999; Pollock et al., 2020). Further elucidation of the molecular mechanisms underlying fibrinogen-mediated NLRP3 priming and inhibition via knockdown of fibrinogen-binding receptors is required to determine whether phagocytosis or receptor-mediated signaling is primarily driving microglia priming.

In addition to their role as cell-cell communicators, brain derived EVs including those released from microglia make promising indicators of cellular activity since they readily cross the BBB and can be detected in the peripheral circulation. This property of EVs has enabled plasma-based measurements of neuronal and astrocytic EVs carrying disease-related cargo, but has not been applied for the detection of EVs indicative of BBB disruption. (Goetzl et al., 2016; Winston et al., 2016) In this study, an experimental stroke model was used to investigate whether EVs reflective of BBB dysfunction and microglial activity can also be detected peripherally. Following a focal injection of endothelin-1, the release of signaling molecules induced by ischemia are responsible for an increase in BBB permeability (Fischer et al., 1999; Chen et al., 2000). Twenty-eight days post stroke there was evidence of fibrinogen uptake by microglia cells in the lesion site, which was mirrored by an increase in circulating EVs dual-labelled with fibrinogen and the microglial protein TMEM119. Previous experimental models of stroke have demonstrated increased permeability of the BBB that persists up to 14 days post-stroke, and up to 3-months following subcortical stroke in human patients (Durukan et al., 2009; Yang et al., 2015; Morgan et al., 2020). This represents a novel method of tracking BBB dysfunction by harnessing the association between fibrinogen extravasation, microglia activity and EV release that was identified in our in vitro models. Currently, the detection of BBB dysfunction and microglia activity in vivo are limited to advanced neuroimaging techniques and further development of EV-based targets would enable more sophisticated and non-invasive measurement in human and experimental disease models. This represents a critical step for identifying, and potentially modifying, microglia activity given the known associations between microglia activation and cognitive impairment in aging, Alzheimer's disease and stroke (Levit et al., 2019, 2021). Furthermore, fibrinogen carrying EVs released from microglia in response to BBB leakiness that are pro-inflammatory in nature may represent a link between chronic microglia activity and the peripheral inflammatory system.

In conclusion, our in vitro work suggests an interplay between pro-inflammatory microglia activity, fibrinogen signaling and EV-mediated cell communication and a proposed mechanism is presented in Fig. 5. Importantly, in vivo validation of these mechanisms is required to better elucidate how fibrinogen and NLRP3 signaling influence the response to neurological disease. These results are relevant to multiple neurological conditions given that BBB disruption is persistent following acute neurological injury and occurs early in the trajectory of chronic neurodegenerative diseases (Ujiie et al., 2003; Hay et al., 2015). As a result of BBB dysfunction, fibrinogen may act as the stimulus for NLRP3 driven release of pro-inflammatory EVs from microglia that affect not only neighboring microglia but other glial cells and neurons as well. Future work investigating the implications of EVs released from microglia following fibrinogen exposure, their utility as circulating indicators of BBB dysfunction, and pharmacological inhibition of these pathways is required.

Ethics approval

All animal procedures were approved by the Animal Care Committee at Western University (protocol 2018–132). All rats used in this study were housed in facilities maintained by Western University Animal Care and Veterinary Services.

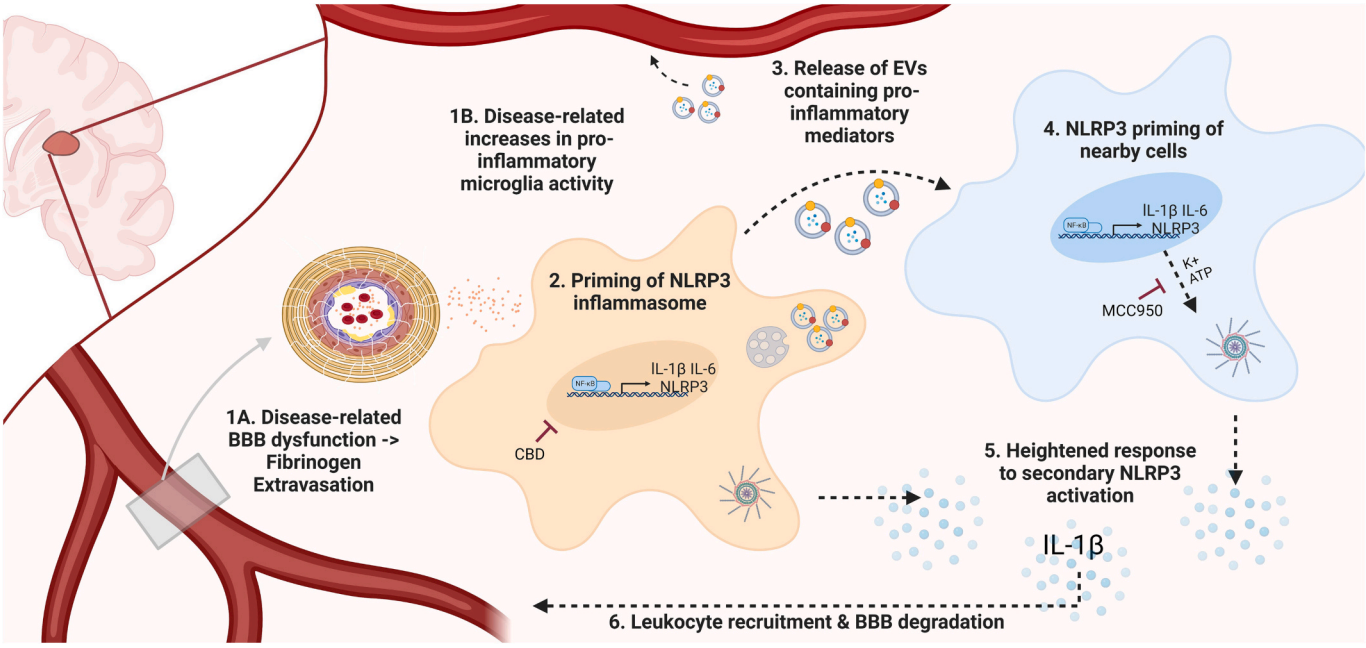

Fig. 5. Schematic of potential interactions between BBB dysfunction, microglia NLRP3 inflammasome activity and EV-propagated signaling. 1) Age-related increases in both ongoing microglia activity and BBB leakiness 2) Fibrinogen extravasation upregulates transcription of pro-inflammatory mediators and NLRP3 inflammasome components 3) NLRP3 priming results in increase of EVs containing fibrinogen and pro-inflammatory mediators which can enter the blood stream or be taken up by nearby cells (through phagocytosis, membrane fusion, etc.) 4) NLRP3 priming of recipient cells 5) Additional stimulation of the NLRP3 inflammasome via K+/ ATP following stress such as ischemia leads to heightened release of pro-inflammatory cytokines, 6) pro-inflammatory cytokines such as IL-1β, TNF-α promote leukocyte recruitment and further degradation of the BBB. Figure created with BioRender.com

Availability of data and materials

The datasets used and/or analyzed during the current study are available from the corresponding author on reasonable request.

CRediT authorship contribution statement

A.D. Roseborough: Conceptualization, Investigation, Formal analysis, Visualization, Writing – original draft. **Y. Zhu:** Investigation, Methodology. **L. Zhao:** Conceptualization, Methodology. **S.R. Laviolette:** Methodology, Writing - review & editing. **S.H. Pasternak:** Conceptualization, Writing – review & editing. **S.N. Whitehead:** Conceptualization, Supervision, Resources, Writing – review & editing, Funding acquisition.

Declaration of Competing Interest

The authors declare no competing interests.

Data availability

Data will be made available on request.

Acknowledgements

Authors received funding support from Canadian Institute of Health Research to ADR and SNW, Ontario Graduate Scholarship to SJM, Canadian Consortium for Neurodegeneration in Aging, Canadian Foundation for Innovation, and Natural Sciences and Engineering Council of Canada, Western University Interdisciplinary Initiative to SNW. SHP receives funding support from the Weston Brain Institute and Zywie Bio LLC.

Appendix A. Supplementary data

Supplementary data to this article can be found online at https://doi.org/10.1016/j.nbd.2023.106001.

References

Agalave, N.M., Lane, B.T., Mody, P.H., Szabo-Pardi, T.A., Burton, M.D., 2020. Isolation, culture, and downstream characterization of primary microglia and astrocytes from adult rodent brain and spinal cord. J. Neurosci. Methods 340. https://doi.org/10.1016/j.jneumeth.2020.108742, 108742 Available at:

Ballabh, P., Braun, A., Nedergaard, M., 2004. The blood-brain barrier: an overview: structure, regulation, and clinical implications. Neurobiol. Dis. 16, 1–13.

Banks, W.A., 2008. The blood brain barrier. Neuroimmune Pharmacol 21–38.

Bridges, L.R., Andoh, J., Lawrence, A.J., Khoong, C.H.L., Poon, W.W., Esiri, M.M., Markus, H.S., Hainsworth, A.H., 2014. Blood-brain barrier dysfunction and cerebral small vessel disease (arteriolosclerosis) in brains of older people. J. Neuropathol. Exp. Neurol. 73, 1026–1033. Available at: http://journals.lww.com/jneuropath/Fulltext/2014/11000/Blood_Brain_Barrier_Dysfunction_and_Cerebral_Small.5.aspx.

Budden, C.F., Gearing, L.J., Kaiser, R., Standke, L., Hertzog, P.J., Latz, E., 2021. Inflammasome-induced extracellular vesicles harbour distinct RNA signatures and alter bystander macrophage responses. J Extracell Vesicles 10.

Chen, Y., McCarron, R.M., Azzam, N., Bembry, J., Reutzler, C., Lenz, F.A., Spatz, M., 2000. Endothelin-1 and nitric oxide affect human cerebromicrovascular endothelial responses and signal transduction. Acta Neurochir. 76, 131–135.

Coll, R.C., et al., 2015. A small-molecule inhibitor of the NLRP3 inflammasome for the treatment of inflammatory diseases. Nat. Med. 21, 248–257.

Davalos, D., Kyu Ryu, J., Merlini, M., Baeten, K.M., Le Moan, N., Petersen, M.A., Deerinck, T.J., Smirnoff, D.S., Bedard, C., Hakozaki, H., Gonias Murray, S., Ling, J. B., Lassmann, H., Degen, J.L., Ellisman, M.H., Akassoglou, K., 2012. Fibrinogen-induced perivascular microglial clustering is required for the development of axonal damage in neuroinflammation. Nat Commun 3, 1227. Available at. https://doi.org/10.1038/ncomms2230.

Dempsey, C., Rubio Araiz, A., Bryson, K.J., Finucane, O., Larkin, C., Mills, E.L., Robertson, A.A.B., Cooper, M.A., O'Neill, L.A.J., Lynch, M.A., 2017. Inhibiting the NLRP3 inflammasome with MCC950 promotes non-phlogistic clearance of amyloid-β and cognitive function in APP/PS1 mice. Brain Behav. Immun. 61, 306–316.

Durukan, A., Marinkovic, I., Strbian, D., Pitkonen, M., Pedrono, E., Soinne, L., Abo-Ramadan, U., Tatlisumak, T., 2009. Post-ischemic blood–brain barrier leakage in rats: one-week follow-up by MRI. Brain Res. 1280, 158–165. Available at: https://www.sciencedirect.com/science/article/pii/S0006899309009585.

Feuerstein, G.Z., Liu, T., Barone, F.C., 1994. Cytokines, inflammation, and brain injury: role of tumor necrosis factor-alpha. Cerebrovasc. Brain Metab. Rev. 6, 341–360.

Fischer, S., Clauss, M., Wiesnet, M., Renz, D., Schaper, W., Karliczek, G.F., 1999. Hypoxia induces permeability in brain microvessel endothelial cells via VEGF and NO. Am. J. Phys. 276, C812–C820.

Goetzl, E.J., Mustapic, M., Kapogiannis, D., Eitan, E., Lobach, I.V., Goetzl, L., Schwartz, J. B., Miller, B.L., 2016. Cargo proteins of plasma astrocyte-derived exosomes in Alzheimer's disease. FASEB J. 30, 3853–3859.

Hay, J.R., Johnson, V.E., Young, A.M.H., Smith, D.H., Stewart, W., 2015. Blood-brain barrier disruption is an early event that may persist for many years after traumatic brain injury in humans. J. Neuropathol. Exp. Neurol. 74, 1147–1157.

Horvath, R.J., Nutile-McMenemy, N., Alkaitis, M.S., DeLeo, J.A., 2008. Differential migration, LPS-induced cytokine, chemokine, and NO expression in immortalized BV-2 and HAPI cell lines and primary microglial cultures. J. Neurochem. 107, 557–569.

Iraci, N., Leonardi, T., Gessler, F., Vega, B., Pluchino, S., 2016. Focus on extracellular vesicles: physiological role and signalling properties of extracellular membrane vesicles. Int. J. Mol. Sci. 17.

Ismael, S., Zhao, L., Nasoohi, S., Ishrat, T., 2018. Inhibition of the NLRP3-inflammasome as a potential approach for neuroprotection after stroke. Sci. Rep. 8, 1–9.

Janelidze, S., Hertze, J., Nägga, K., Nilsson, K., Nilsson, C., Wennström, M., van Westen, D., Blennow, K., Zetterberg, H., Hansson, O., 2017. Increased blood-brain barrier permeability is associated with dementia and diabetes but not amyloid pathology or APOE genotype. Neurobiol. Aging 51, 104–112. Available at: https://www.sciencedirect.com/science/article/pii/S0197458016303049.

Jenkins, D.R., Craner, M.J., Esiri, M.M., DeLuca, G.C., 2018. Contribution of fibrinogen to inflammation and neuronal density in human traumatic brain injury. J. Neurotrauma 35, 2259–2271.

Koellhoffer, E.C., McCullough, L.D., Ritzel, R.M., 2017. Old maids: aging and its impact on microglia function. Int. J. Mol. Sci. 18, 1–25.

Kozela, E., Pietr, M., Juknat, A., Rimmerman, N., Levy, R., Vogel, Z., 2010. Cannabinoids Δ9-tetrahydrocannabinol and cannabidiol differentially inhibit the lipopolysaccharide-activated NF-κB and interferon-β/STAT proinflammatory pathways in BV-2 microglial cells. J. Biol. Chem. 285, 1616–1626.

Lee, S.J., Hong, J.M., Lee, S.E., Kang, D.R., Ovbiagele, B., Demchuk, A.M., Lee, J.S., 2017. Association of fibrinogen level with early neurological deterioration among acute ischemic stroke patients with diabetes. BMC Neurol. 17, 1–7.

Levit, A., Regis, A.M., Gibson, A., Hough, O.H., Maheshwari, S., Agca, Y., Agca, C., Hachinski, V., Allman, B.L., Whitehead, S.N., 2019. Impaired behavioural flexibility related to white matter microgliosis in the TgAPP21 rat model of Alzheimer disease. Brain Behav. Immun. 80, 25–34. Available at: https://doi.org/10.1016/j.bbi.2019.02.013.

Levit, A., Gibson, A., Hough, O., Jung, Y., Agca, Y., Agca, C., Hachinski, V., Allman, B.L., Whitehead, S.N., 2021. Precocious white matter inflammation and Behavioural inflexibility precede learning and memory impairment in the TgAPP21 rat model of Alzheimer disease. Mol 58, 5014–5030.

Livak, K.J., Schmittgen, T.D., 2001. Analysis of relative gene expression data using real-time quantitative PCR and the 2(-Delta Delta C(T)) method. Methods 25, 402–408.

MacKenzie, A., Wilson, H.L., Kiss-Toth, E., Dower, S.K., North, R.A., Surprenant, A., 2001. Rapid secretion of interleukin-1β by microvesicle shedding. Immunity 15, 825–835. Available at: https://www.sciencedirect.com/science/article/pii/S1074761301002291.

McAleese, K.E., Graham, S., Dey, M., Walker, L., Erskine, D., Johnson, M., Johnston, E., Thomas, A.J., McKeith, I.G., DeCarli, C., Attems, J., 2019. Extravascular fibrinogen in the white matter of Alzheimer's disease and normal aged brains: implications for fibrinogen as a biomarker for Alzheimer's disease. Brain Pathol. 29, 414–424.

Merlini, M., Rafalski, V.A., Coronado, P.E.R., Mucke, L., Nelson, R.B., Merlini, M., Rafalski, V.A., Coronado, P.E.R., Gill, T.M., Ellisman, M., Muthukumar, G., 2019. Fibrinogen induces microglia-mediated spine elimination and cognitive impairment in an Alzheimer ' s disease model report fibrinogen induces microglia-mediated spine elimination and cognitive impairment in an Alzheimer ' s disease model. Neuron 101. https://doi.org/10.1016/j.neuron.2019.01.014, 1099-1108.e6 Available at.

Montagne, A., Barnes, S.R., Sweeney, M.D., Halliday, M.R., Sagare, A.P., Zhao, Z., Toga, A.W., Jacobs, R.E., Liu, C.Y., Amezcua, L., Harrington, M.G., Chui, H.C., Law, M., Zlokovic, B.V., 2015. Blood-brain barrier breakdown in the aging human Hippocampus. Neuron 85, 296–302.

Montagne, A., et al., 2018. Pericyte degeneration causes white matter dysfunction in the mouse central nervous system. Nat. Med. 24, 326–337. Available at: http://ovidsp.ovid.com/ovidweb.cgi?T=JS&PAGE=reference&D=prem&NEWS=N&AN=29400711.

Morgan, C.A., Mesquita, M., Ashioti, M., Beech, J.S., Williams, S.C.R., Irving, E., Cash, D., 2020. Late changes in blood–brain barrier permeability in a rat tMCAO model of stroke detected by gadolinium-enhanced MRI. Neurol. Res. 42, 844–852. Available at: https://doi.org/10.1080/01616412.2020.1786637.

Nham, S.U., 1999. Characteristics of fibrinogen binding to the domain of CD11c, an alpha subunit of p150,95. Biochem. Biophys. Res. Commun. 264, 630–634.

Osteikoetxea, X., Sódar, B., Németh, A., Szabó-Taylor, K., Pálóczi, K., Vukman, K.V., Tamási, V., Balogh, A., Kittel, Á., Pállinger, É., Buzás, E.I., 2015. Differential detergent sensitivity of extracellular vesicle subpopulations. Org Biomol Chem 13, 9775–9782.

Petersen, M.A., et al., 2017. Fibrinogen activates BMP signaling in oligodendrocyte progenitor cells and inhibits Remyelination after vascular damage. Neuron 96. https://doi.org/10.1016/j.neuron.2017.10.008, 1003-1012.e7 Available at:

Pollock, T.B., Cholico, G.N., Isho, N.F., Day, R.J., Suresh, T., Stewart, E.S., McCarthy, M. M., Rohn, T.T., 2020. Transcriptome analyses in BV2 microglial cells following

treatment with amino-terminal fragments of apolipoprotein E. Front. Aging Neurosci. 12, 256. Available at: https://pubmed.ncbi.nlm.nih.gov/32922284.
Prakash, R., Carmichael, T., 2015. Blood-brain barrier breakdown and neovascularization processes after stroke and traumatic brain injury. Curr. Opin. Neurol. 28, 556–564.
Raj, D., Yin, Z., Breur, M., Doorduin, J., Holtman, I.R., Olah, M., Mantingh-otter, I.J., Van, Dam D., De, Deyn P.P., Den, Dunnen W., Eggen, B.J.L., Amor, S., Boddeke, E., 2017. Increased White Matter Inflammation in Aging- and Alzheimer's Disease Brain, 10, pp. 1–18.
Raja, R., Rosenberg, G.A., Caprihan, A., 2018. MRI measurements of blood-brain barrier function in dementia: a review of recent studies. Neuropharmacology 134, 259–271. Available at: https://www.sciencedirect.com/science/article/pii/S0028390817305014.
Ravichandran, K.A., Heneka, M.T., 2021. Inflammasome activation in neurodegenerative diseases. Essays Biochem. 65, 885–904.
Roseborough, A.D., Rasheed, B., Jung, Y., Nishimura, K., Pinsky, W., Langdon, K.D., Hammond, R., Pasternak, S.H., Khan, A.R., Whitehead, S.N., 2021. Microvessel stenosis, enlarged perivascular spaces, and fibrinogen deposition are associated with ischemic periventricular white matter hyperintensities. Brain Pathol 1–13.
Ryu, J.K., McLarnon, J.G., 2009. A leaky blood-brain barrier, fibrinogen infiltration and microglial reactivity in inflamed Alzheimer's disease brain. J. Cell. Mol. Med. 13, 2911–2925.
Schoknecht, K., Shalev, H., 2012. Blood-brain barrier dysfunction in brain diseases: clinical experience. Epilepsia 53 (Suppl. 6), 7–13.
Senatorov, V.V., et al., 2019. Blood-brain barrier dysfunction in aging induces hyperactivation of TGFβ signaling and chronic yet reversible neural dysfunction. Sci. Transl. Med. 11.
Swanson, K.V., Deng, M., Ting, J.P.Y., 2019. The NLRP3 inflammasome: molecular activation and regulation to therapeutics. Nat Rev Immunol 19, 477–489. Available at: https://doi.org/10.1038/s41577-019-0165-0.
Sweeney, M.D., et al., 2019. Vascular dysfunction-the disregarded partner of Alzheimer's disease. Alzheimers Dement. 15, 158–167.
Thrippleton, M.J., Backes, W.H., Sourbron, S., Ingrisch, M., van Osch, M.J.P., Dichgans, M., Fazekas, F., Ropele, S., Frayne, R., van Oostenbrugge, R.J., Smith, E.E., Wardlaw, J.M., 2019. Quantifying blood-brain barrier leakage in small vessel disease: review and consensus recommendations. Alzheimers Dement. 15, 840–858. Available at: https://pubmed.ncbi.nlm.nih.gov/31031101.
Ujiie, M., Dickstein, D.L., Carlow, D.A., Jefferies, W.A., 2003. Blood-brain barrier permeability precedes senile plaque formation in an Alzheimer disease model. Microcirculation 10, 463–470.
Verheggen, I.C.M., de Jong, J.J.A., van Boxtel, M.P.J., Gronenschild, E.H.B.M., Palm, W. M., Postma, A.A., Jansen, J.F.A., Verhey, F.R.J., Backes, W.H., 2020a. Increase in blood – brain barrier leakage in healthy, older adults. GeroScience 42, 1183–1193.
Verheggen, I.C.M., de Jong, J.J.A., van Boxtel, M.P.J., Postma, A.A., Jansen, J.F.A., Verhey, F.R.J., Backes, W.H., 2020b. Imaging the role of blood-brain barrier disruption in normal cognitive ageing. GeroScience 42, 1751–1764.
Viggars, A.P., Wharton, S.B., Simpson, J.E., Matthews, F.E., Brayne, C., Savva, G.M., Garwood, C., Drew, D., Shaw, P.J., Ince, P.G., 2011. Alterations in the blood brain barrier in ageing cerebral cortex in relationship to Alzheimer-type pathology: a study in the MRC-CFAS population neuropathology cohort. Neurosci. Lett. 505, 25–30. Available at: https://doi.org/10.1016/j.neulet.2011.09.049.
Vilar, R., Fish, R.J., Casini, A., Neerman-Arbez, M., 2020. Fibrin(ogen) in human disease: both friend and foe. Haematologica 105, 284–296.
Winston, C.N., Goetzl, E.J., Akers, J.C., Carter, B.S., Rockenstein, E.M., Galasko, D., Masliah, E., Rissman, R.A., 2016. Prediction of conversion from mild cognitive impairment to dementia with neuronally derived blood exosome protein profile. Alzheimer's Dement (Amsterdam, Netherlands) 3, 63–72.
Xu, G., Zhang, H., Zhang, S., Fan, X., Liu, X., 2008. Plasma fibrinogen is associated with cognitive decline and risk for dementia in patients with mild cognitive impairment. Int. J. Clin. Pract. 62, 1070. –1075 Available at: https://doi.org/10.1111/j.1742-1241.2007.01268.x.
Yang, J., d'Esterre, C., Ceruti, S., Roversi, G., Saletti, A., Fainardi, E., Lee, T.Y., 2015. Temporal changes in blood–brain barrier permeability and cerebral perfusion in lacunar/subcortical ischemic stroke. BMC Neurol. 15, 214. Available at: https://doi.org/10.1186/s12883-015-0468-0.
Zhang, Y., Liu, F., Yuan, Y., Jin, C., Chang, C., Zhu, Y., Zhang, X., Tian, C., He, F., Wang, J., 2017. Inflammasome-derived exosomes activate NF-κB signaling in macrophages. J. Proteome Res. 16, 170–178.